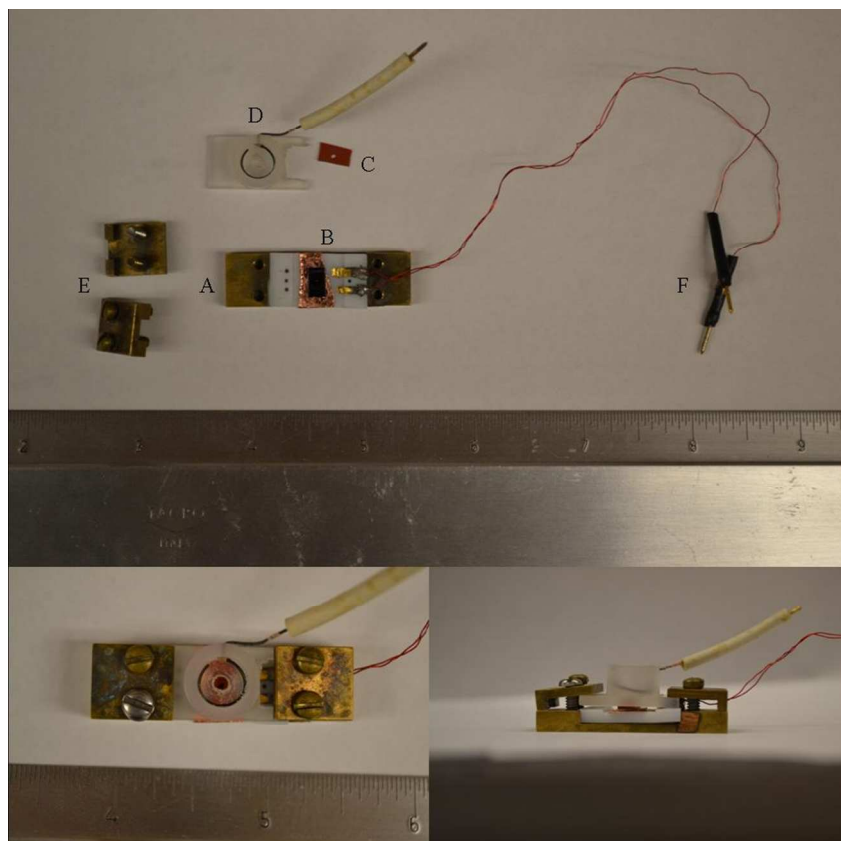Supporting Information

Electropolymerization of Poly(phenylene oxide) on Graphene as a Top-Gate Dielectric

Alexey Lipatov,[#] Benjamin B. Wymore,[#] Alexandra Fursina, Timothy H. Vo, Alexander Sinitskii,* and Jody G. Redepenning*

Department of Chemistry, University of Nebraska – Lincoln, Lincoln, Nebraska 68588, United States

Figure S1. Cell used for the electrodeposition of PPO on lithographically patterned wafers. **(a)** Top view of cell components: The wafer was secured on the sample holder, A, with copper double sided tape. Electrical connection to the wafer was made by ultrasonically welding 0.0025 inch gold wire onto the wafer and gold pads, B, that were connected to external wires, F, for simple potentiostat attachment. A silicone gasket, C, was placed on top of the wafer exposing the desired area for electrodeposition. The reservoir, D, was placed on top of the gasket which maintained exposure. The reservoir was fastened in place with copper clamps, E, that were lightly tightened to prevent leakage of the solution. Images of the constructed cell from the **(b)** top and the **(c)** side views are shown.

PPO film characterization.

A way to determine the existence of pinholes within the PPO is to perform cyclic voltammetry on a redox couple. If the pinholes in a thin film passivating an electrode are close together, the shape of the CV for a dissolved redox couple resembles the shape of the CV for the same redox couple at a bare electrode, but with a smaller peak current. If the pinholes are spaced far enough apart such that their diffusion layers do not overlap during the potential sweep, then the CV waveshape for a dissolved redox couple resembles the waveshape for a steady-state mass transfer limited voltammogram. The pinholes act as a collection of ultramicroelectrodes, where the diffusion layer thickness is large compared to the size of the ultramicroelectrode (pinhole). If there are no pinholes within the film, then there is no Faradaic current during the potential sweep.[1,2]

Figure S2 shows CVs of an aqueous solution containing 5 mM hexaammineruthenium(III) chloride ($Ru(NH_3)_6Cl_3$) and 1 M potassium chloride (KCl) at a glassy carbon electrode with and without PPO. $Ru(NH_3)_6^{3+}$ has a hydrated radius of 0.64 nm at 22°C.[3] The PPO was deposited using a variety deposition conditions. The maximum switching potential of the working electrode and number of potential cycles used during the deposition of PPO were adjusted to determine the optimum conditions for the production of pinhole free films. Figure S2a compares PPO films prepared by cycling the potential 90 times between the following potentials: 0 V to 1 V, 0 V to 1.1 V, and 0 V to 1.2 V. The deposition with a maximum switching potential of 1.1 V vs. SCE resulted in the lowest reduction peak current for the $Ru(NH_3)_6^{3+}$, and the voltammogram approaches the shape expected for steady state mass transfer. This indicates that the pinholes in the film are separated by large distances and that the diffusion layers of the pinholes do not overlap. Figure S2b shows the same CV comparison but with PPO films deposited onto the electrode with 180 potential cycles. Again, films prepared using a maximum switching potential of 1.1 V resulted in the lowest reduction peak current. The film prepared with 90 potential cycles does not passivate the electrode as well as the 180 potential cycles and indicates that more potential cycles are needed to improve the film passivation.

Evidence presented in the scientific literature may explain the differences in the degree of passivation that arises when different PPO deposition voltages are used. When studying PPO films that were deposited by passing the same amount of charge but at different potentials, McCarley et al.[4] found that PPO films deposited at mild potentials act as transport barriers but not as well as the films prepared at highly anodic potentials. These researchers postulated that at highly positive potentials, additional polymerization mechanisms might further oxidize the films to produce cross-linked structures. The decrease in the barrier effectiveness when 1.2 V is applied may be due to film decomposition.[5]
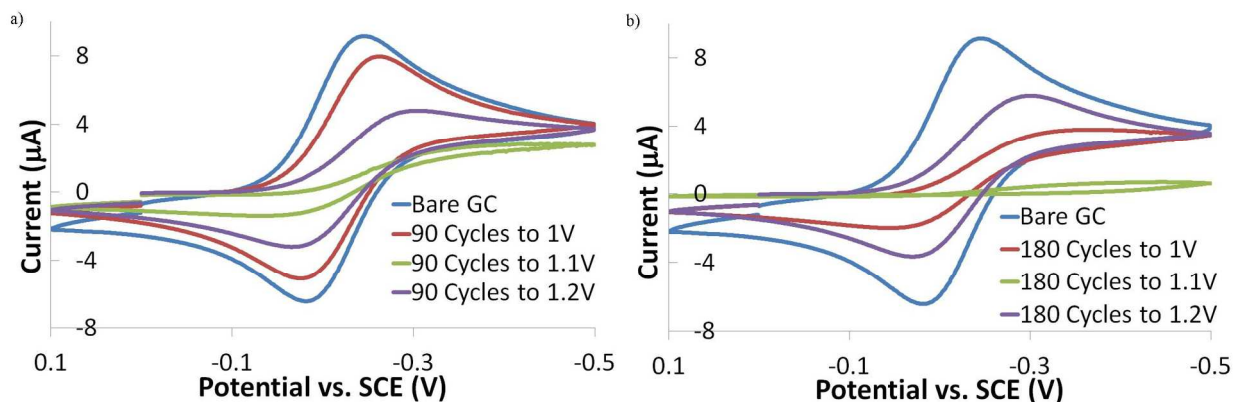
Figure S2: Comparison of the PPO films prepared from the aqueous solution containing 50 mM phenol and 0.5 M H_2SO_4 with **(a)** 90 potential cycles, and **(b)** 180 potential cycles to different maximum potentials in $Ru(NH_3)_6^{3+}$ solution.

Rhodes et al.[1] observed further passivation of their electrodes after annealing their films at 150°C in vacuum. They postulated that the increase in passivation was due to crosslinking within the film or chain reorganization and packing effects. Figure S3 compares voltammetric responses to 5 mM $Ru(NH_3)_6^{3+}$ at a bare Au coated wafer, after PPO deposition (90 potential cycles from 0 V to 1.1 V) on a gold coated wafer, and after annealing the wafer at 150°C for 15 hours in vacuum. The electrode area available to the solution is much smaller at the PPO coated electrode than at the bare Au wafer, but it is clear that the passivating layer does not completely block the redox species from reaching the electrode surface. The electrode appears fully blocking to 5 mM $Ru(NH_3)_6^{3+}$ after annealing the wafer, in agreement with the results reported by Rhodes.
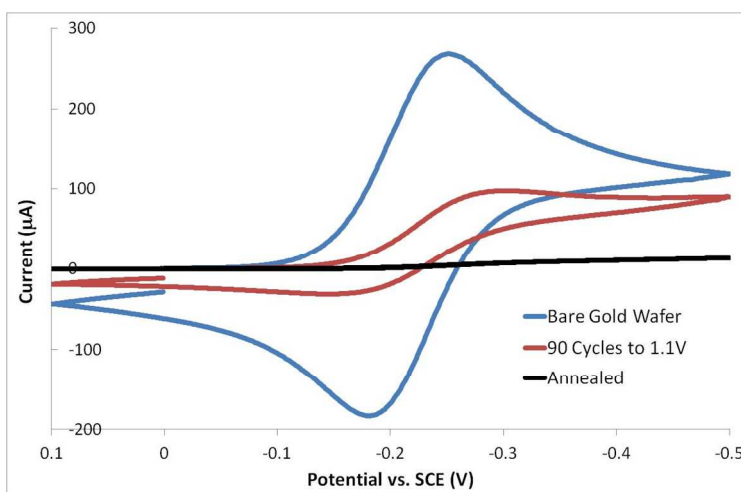
Figure S3: CV characterization of the PPO film grown on a gold wafer before and after annealing.

3
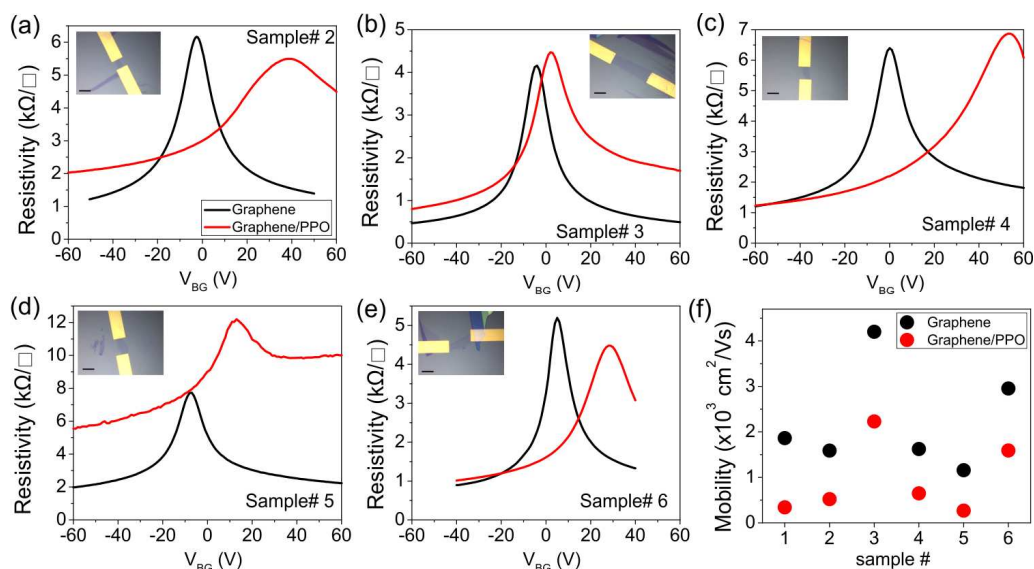
Figure S4: **(a-e)** Optical images (scale bar is 10 µm) and transfer characteristics for 5 devices before (black) and after (red) PPO deposition. **(f)** Mobility values for graphene devices presented in (a-c) as well as sample from the main text (sample #1) before and after PPO deposition.

Variability in sheet resistivity for exfoliated graphene devices before and after electrodeposition of PPO.

Found below is a more detailed statistical analysis of the device-to-device variability in the sheet resistances for exfoliated graphene devices shown in Figure 3(b). Note that the resistivity for device #5 in Figure 3(b) looks anomalous, especially so when one examines the last column (Resistivity Change) of the Table found below.

Sample #	Resistivity Graphene (all data)	Resistivity Graphene/PPO (all data)	Resistivity Change
1	2631	3270	639
2	6167	5496	-671
3	4159	4470	311
4	6393	6870	477
5	7726	12198	4472
6	5194	4480	-714
Mean	5378	6131	752
St. Dev.	1802	3207	1913
RSD (%)	34	52	254

We performed the well-recognized Grubb's test for outliers focused on the resistivity change for devices #5.[6]

The result is:
$$G_{data} = \frac{x_{max} - \bar{x}}{s} = \frac{4472 - 752}{1913} = 1.945,$$

where x_{max} is the data point in question, $\bar{x}$ is the average for the data set (including the point in question), and s is the standard deviation of the data set (including the point in question).

The critical value of G for this number of data points is 1.887 at the 95% confidence level; therefore, we treat PPO-coated device # 5 as an outlier ($P < 0.05$) and re-treat the data as shown below.

Sample #	Resistivity Graphene (all data)	Resistivity Graphene/PPO (minus outlier)	Resistivity Change (minus outlier)
1	2631	3270	639
2	6167	5496	-671
3	4159	4470	311
4	6393	6870	477
5	7726		
6	5194	4480	-714
Mean	5378	4917	8
s	1802	1346	650
rsd(%)	34	27	

A paired student t-test (not shown) of these data sets does not reveal a significant difference in the sheet resistance of the graphene and PPO-coated graphene. Furthermore, the resistivity change (after removing the outlier) is not significantly different from zero.

Thickness control

Although we can control film thickness with the number of cycles and the potential to which the graphene is cycled, it is not presently possible for us to eliminate pinholes for films thinner than approximately 2 nm (using a small number of cycles or an anodic potential limit that is not very positive). Under the conditions we describe here, the films self-limit to a thickness of approximately 5 nm. We have investigated a large number of conditions, none of which are described here, which lead to PPO thicknesses greater than 10 nm. Some of these films approach 100 nm in thickness. For one or more reasons, such films are not useful as a dielectric. To give the readers a better sense of film thicknesses achieved under the conditions we do describe here, we show film thicknesses for six devices in Table S5. $\bar{x} \pm 1s$ for these six points is 3.5 ± 0.7

nm. Note that the uncertainty in the thickness of these films is predominantly determined by the uncertainty in the AFM thickness measurement.

Table S5. PPO thickness for 6 devices shown on Figure S4. Sample #1 is from the main text.

Sample #	Height		
	Graphene	Graphene/PPO	PPO
1	1.4(4)	5.0(6)	3.6(7)
2	1.7(3)	5.4(6)	3.7(5)
3	2.1(4)	6.1(7)	4.0(8)
4	2.7(5)	5.5(5)	2.8(7)
5	2.0(4)	4.4(5)	2.4(6)
6	1.4(3)	5.8(6)	4.4(6)
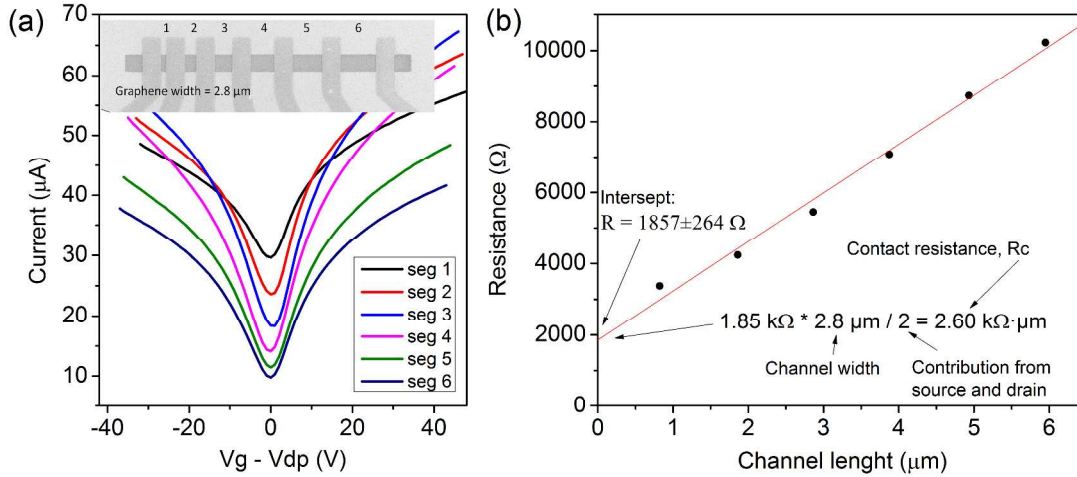
Figure S6: Determination of contact resistance exfoliated graphene using the transfer length method (TLM). **(a)** Transfer characteristics of 6 graphene FETs. **Inset**: SEM image of a graphene FET array consisting of six devices with channel lengths varying from 1 to 6 µm, in steps of 1 µm. **(b)** Calculation of contact resistance using the TLM at the Dirac point. Black dots, measured total resistance; red line, linear fitting curve.
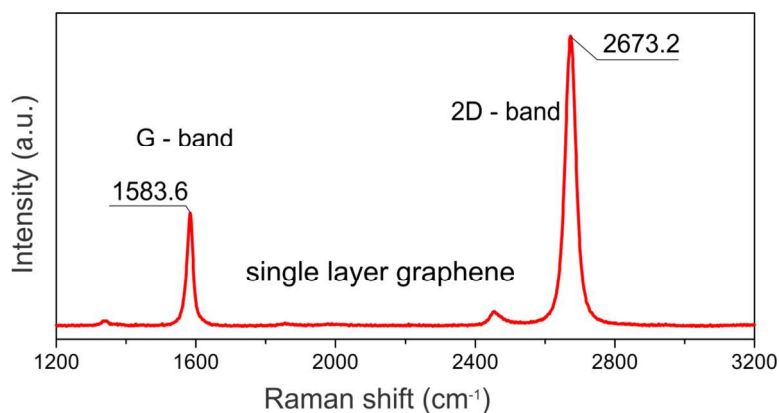
Figure S7: Raman spectrum of single layer graphene on Si/SiO$_2$ wafer used fabricate graphene device array.
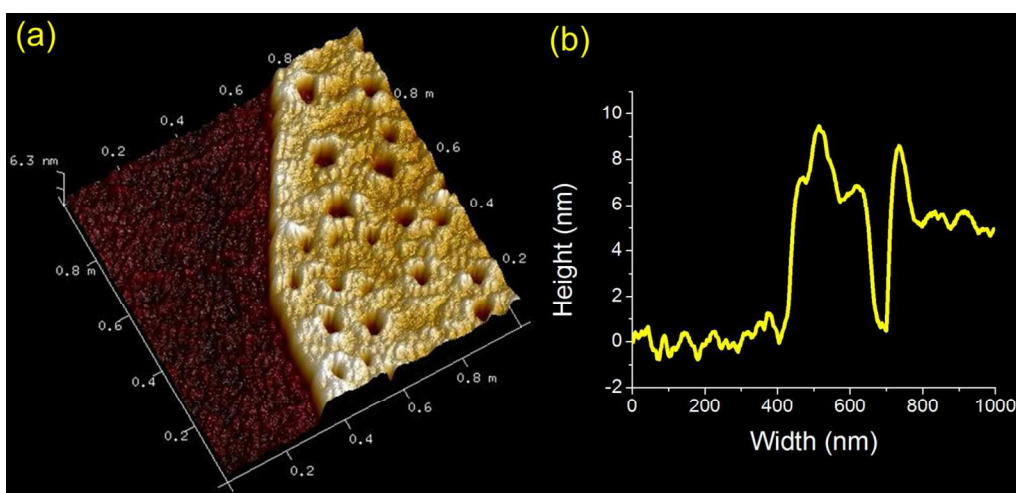
Figure S8: Pores development in the graphene during electropolymerization. **(a)** AFM image of graphene/PPO with holes. **(b)** Height profile of graphene/PPO in (a) which shows the depth of the holes within the PPO film.

References:

(1) Rhodes, C. P.; Long, J. W.; Doescher, M. S.; Fontanella, J. J.; Rolison, D. R. *J. Phys. Chem. B* **2004,** *108*, 13079-13087.
(2) Bard, A. J.; Faulkner, L. R. *Electrochemical Methods: Fundamentals and Applications;* John Wiley & Sons: 2000.
(3) Chailapakul, O.; Crooks, R. M. *Langmuir* **1995,** *11*, 1329-1340.
(4) Mccarley, R. L.; Thomas, R. E.; Irene, E. A.; Murray, R. W. *J. Electroanal. Chem.* **1990,** *290*, 79-92.
(5) Gattrell, M.; Kirk, D. W. *J. Electrochem. Soc.* **1993,** *140*, 903-911.
(6) Grubbs, F. E. *Technometrics* **1969,** *11*, 1-21.